

A Mössbauer effect study of franklinite from Sterling Hill, New Jersey*

E. DE GRAVE¹, R. VOCHTEN², and R. E. VANDENBERGHE¹

¹Department of Subatomic and Radiation Physics, University of Gent, B-9000 Gent, Belgium

²Laboratory of Physical and Chemical Mineralogy, Department of Chemistry, University of Antwerp, B-2020 Antwerp, Belgium

Abstract—Franklinite crystals from the Sterling Hill deposit (Ogdenburg, New Jersey, U.S.A.) have been characterized by X-ray diffraction and atomic absorption spectrometry. The composition of this ferrite was determined to be $Zn_{0.68}Mn_{0.36}Fe_{1.96}O_4$. Mössbauer spectra were recorded at temperatures between 4.3 and 480 K, and at selected low temperatures in the presence of external magnetic fields up to 60 kOe. Both the paramagnetic and the magnetically split spectra consistently reveal that ≈ 0.06 Fe atoms per formula unit are located on the A sites. The doublet spectra are adequately described as a superposition of an Fe^{3+} A-site doublet and two Fe^{3+} B-site doublets, the latter having quadrupole splittings close to the values reported for $ZnFe_2O_4$ and $MnFe_2O_4$, respectively. This finding could be related to the previously suggested presence of Mn- and Zn-rich clusters. Slightly but consistently better fits were obtained using an A-site doublet and a quasi-continuous distribution of quadrupole splittings for the B sites. At temperatures below 245 K and down to ≈ 20 K, the spectral envelope is complex and not entirely interpretable by either static or dynamic (relaxation) effects. The spectra recorded at 4.3 and 9 K exhibit significant asymmetry in peak depths for corresponding pairs of lines. Applied-field Mössbauer spectra reveal the existence of locally canted spin states and reversed B-site spins. Both phenomena cease to exist at a temperature of 30 K and indicate a re-entrant ferrimagnetic state. The predominant B-site sub-pattern is asymmetrical and was reproduced adequately assuming a random angle α between the hyperfine field and the principal axis of the electric field gradient. Additional distributions on the effective hyperfine fields were introduced to interpret the applied-field spectra at 14 and 30 K. The models permitted the determination of the B-site dipolar-field contribution, *i.e.* -8 ± 2 kOe. The quadrupole splitting was found to be negative, and its magnitude is in line with the average value of the paramagnetic quadrupole-splitting distributions. The existence of locally canted spin states implies that in zero applied field the angle α is also fluctuating, and the observed asymmetry in the spectra at 4.3 and 9 K could be explained accordingly. It was further experienced that annealing of the sample at 600°C in vacuum did not produce substantially different Mössbauer spectra.

INTRODUCTION

FRANKLINITE IS a naturally occurring Mn-Zn ferrite with a cubic spinel structure (space group $Fd\bar{3}m$). Franklinite crystals from the Sterling Hill (Ogdenburg, New Jersey, U.S.A.) deposit are known to have been crystallized at extremely low cooling rates (METSGER *et al.*, 1958). According to VOGEL *et al.* (1976), this slow cooling process could have resulted in a clustering of the tetrahedral Mn and Zn cations. Such a clustering effect could explain why the room-temperature (RT) Mössbauer spectra (MS), measured for five franklinite samples, could be interpreted in terms of two quadrupole doublets with hyperfine parameters fixed at the values observed for synthetic $ZnFe_2O_4$ (quadrupole splitting $\Delta E_Q = 0.35$ mm/s) and $MnFe_2O_4$ ($\Delta E_Q = 0.58$ mm/s) respectively. A MS recorded at 50 K in a longitudinal external magnetic field of 50 kOe was

also presented. Two components, both arising from octahedral Fe^{3+} , were obvious and reportedly provide direct evidence that some sort of ordering is present in the as-collected samples.

To the best of the authors' knowledge, a detailed temperature-dependent Mössbauer study of franklinite has so far not been published. Such a study is reported in the present paper. An additional objective was to investigate in more detail the effect of clustering, if present in this particular sample, upon the microscopic magnetic properties of the Fe^{3+} cations as reflected in the temperature variations of the Mössbauer parameters.

MATERIAL AND METHODS

The franklinite sample was collected by one of the authors (RV) from the aforementioned deposit. The crystals were embedded in a manganoan-calcite matrix and were recovered from it by treatment in diluted HCl. A qualitative analysis with energy-dispersive X-rays showed Fe, Mn and Zn to be the major, practically sole observable constituents. Al was observed as a minor element. Some crystals were crushed and dissolved in a Na_2O melt to determine the elements Fe, Mn, and Zn by atomic absorp-

* Contribution No SSF95-03-01, Department of Subatomic and Radiation Physics, University of Gent, Belgium.

tion spectrometry. The MS (see next section) did not exhibit any obvious Fe^{2+} component (detection limit estimated as 1% of total iron), and the composition was found to be close to $\text{Zn}_{0.68}\text{Mn}_{0.36}\text{Fe}_{1.96}\text{O}_4$.

X-ray diffraction (XRD) photographs were obtained with a Guinier-Hägg camera (diameter 100 mm), using silicon powder as an internal standard. All the observed reflections could be attributed to the spinel phase. The lattice parameter, calculated as the arithmetic mean from the eight most prominent reflections, was found as $a = 0.8450 \pm 0.0005$ nm, which is in close agreement with relevant literature data for franklinite (METSGER *et al.*, 1958; VOGEL *et al.*, 1976) and for a synthetic Mn-Zn ferrite with similar composition (MORRISH and CLARK, 1975). Powder XRD patterns, recorded with a Co tube, show relatively sharp spinel reflections, with α_1 and α_2 components well separated at higher diffraction angles. Considering the high sensitivity of the lattice parameters towards the Mn/Zn ratio (MORRISH and CLARK, 1975), this observation implies that the cation distribution is fairly homogeneous.

Mössbauer spectra at variable temperatures between 4.2 and 500 K, and at selected low temperatures ($T \leq 60$ K) in a magnetic field of 60 kOe applied parallel to the γ -ray beam, were obtained with a conventional, constant-acceleration spectrometer with triangular reference signal. The data were recorded in 1024 channels (unfolded spectrum). The spectrometer was periodically calibrated using the spectra of either metallic iron or hematite. The velocity increment was approximately 0.01 mm/s per channel for the paramagnetic MS, and 0.045 mm/s for the magnetically split ones. The source was ^{57}Co in a Rh matrix; however all isomer-shift data quoted hereafter refer to metallic iron at RT. The absorber consisted of powdered crystals and had an effective thickness of ≈ 10 mg Fe/cm². Additional measurements at selected temperatures were performed on a sample annealed for 24 hrs. at 600°C in a vacuum of $\approx 10^{-4}$ mbar. Spectra were recorded until an off-resonance count rate of at least 2.10^6 was reached. Unless otherwise stated, all spectra were fitted with superpositions of symmetrical Lorentzian-shaped doublets or sextets. For each doublet the center shift δ , the quadrupole splitting ΔE_Q , and one width parameter Γ were adjusted. For the sextets, only two width parameters were iterated, *viz.* Γ and $\Delta\Gamma$, so that the widths of the outer, middle, and inner absorption lines are given as $\Gamma_1 = \Gamma + 2\Delta\Gamma$, $\Gamma_2 = \Gamma + \Delta\Gamma$, and $\Gamma_3 = \Gamma$ respectively. Center shifts, quadrupole shifts, $2\epsilon_Q$, and magnetic hyperfine fields, H_{hf} , were iterated by non-linear least-squares fitting. Intensity parameters were adjusted by linear regression. However, in many instances it was necessary to employ an asymmetrical line shape for the sextet spectra and some of the variables were constrained in order to obtain reasonable and consistently varying parameter values. More details about this line shape and the constraints will be presented where relevant.

RESULTS AND DISCUSSION

Paramagnetic spectra

The MS recorded at temperatures above 250 K consist of a slightly asymmetric doublet; this asymmetry can be characteristic of a superposition of at least two distinct components with different values

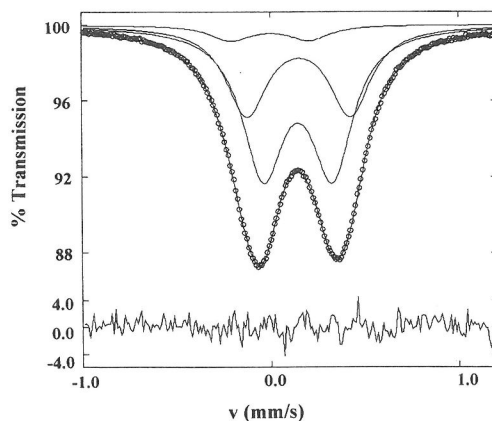


FIG. 1. Mössbauer spectrum (Rh source) of franklinite sample recorded at 470 K. Solid curves are the three quadrupole doublets and their superposition adjusted to the experimental data. The lack of significant structure in the residual (bottom) supports the adequacy of the applied fitting model.

for the hyperfine parameters δ and ΔE_Q . A sample spectrum is shown in Fig.1 ($T = 470$ K) and is representative of spectra for all temperatures in the paramagnetic regime. The full line through the data points is the fitted sum of three symmetrical quadrupole doublets, all assumed to have equal line widths, which are also reproduced in the drawing. The lower part of Fig.1 represents the residual function which obviously lacks any fine structure. This is not the case if only the two predominant quadrupole-split components are employed in the fit. The residual is then not featureless and consistently suggests the presence of a third spectral component. The goodness-of-fit, χ^2 , is typically 25 to 30% lower for a three-doublet fit than for a two-doublet fit. This improvement is statistically significant and is believed to have a physical significance as well.

The quadrupole splittings $\Delta E_{Q,i}$ and the fractional areas A_i ($i = 1,2,3$) of the three doublets, henceforth denoted as D1, D2, and D3, do not vary monotonically with temperature. Their fitted values in the temperature range 260–485 K are scattered between the lower and upper limits listed in Table 1. The line width Γ gradually decreases with increasing T from 0.30 mm/s at 260 K to 0.26 mm/s at 485 K. Such a variation can be explained by the lowering of the Mössbauer fraction, and hence of the effective thickness of the absorber, as the temperature increases (DE GRAVE and VOCHTEN, 1985). Compared to the 260 K spectrum, the line

Table 1. Intervals within which the iterated values of the quadrupole splitting ΔE_Q and of the fractional area A are scattered for the tetrahedral (D3) and two octahedral (D1, D2) doublets fitted to the Mössbauer spectra recorded at temperatures between 260 and 485 K (15 spectra).

	D1	D2	D3
ΔE_Q (mm/s)	0.35-0.38	0.53-0.55	0.30-0.40
A	0.58-0.65	0.31-0.36	0.03-0.08

width of the doublets at 250 K is markedly higher. This broadening implies that the Curie temperature T_C , as probed by the Mössbauer effect, is in the vicinity of 250 K, which is in fair agreement with values reported in the literature for synthetic (Mn, Zn) ferrites with comparable Mn/Zn ratios (see *e.g.* KÖNIG, 1972).

The center shifts of D1 and D2 are consistently equal within experimental error limits (0.358 and 0.363 mm/s respectively at RT), and their values are characteristic of six-fold oxygen coordination in spinel oxides. The quadrupole splittings of the two B-site doublets are indeed very close to those found for Zn and Mn ferrite, respectively. Moreover, the fractional-area ratio A_2/A_1 is comparable with the analytically determined Mn/Zn ratio. These findings, together with the narrow line width of both doublets, suggest that the sample is composed of clusters with fairly uniform compositions close to $ZnFe_2O_4$ and $MnFe_2O_4$. The third doublet has $\delta = 0.24$ mm/s at RT which is typical for a tetrahedral coordination in a spinel ferrite (VANDENBERGHE and DE GRAVE, 1989). This finding implies that the cation distribution in the franklinite studied here exhibits a small degree of inversion with respect to Fe, *i.e.* 0.055 ± 0.025 (see Table 1), in reasonable agreement with the conclusions in that respect put forward by MORRISH and CLARK (1975) for synthetic (Mn, Zn) ferrites. The temperature variation of the B-site center shifts follows normal behavior as expected on the basis of the second-order Doppler shift (DE GRAVE and VAN ALBOOM, 1991). At each temperature, the fitted δ values for the tetrahedral sites are consistently lower by 0.10 to 0.15 mm/s than the corresponding B-site values. The average difference is 0.13 mm/s, which is typical for spinel ferrites (DA COSTA *et al.*, 1994).

All doublet MS have additionally been analyzed

in terms of a model-independent quadrupole-splitting distribution (QSD) with an adjustable linear correlation between δ and ΔE_Q . The latter quantity was allowed to vary in the range 0.1 to 2.0 mm/s in steps of 0.05 mm/s. The value of the smoothing parameter was chosen according to the "first rule of fist" as described by VANDENBERGHE *et al.* (1994). In order to be consistent with the three-doublet model, a non-distributed A-site doublet, with ΔE_Q and Γ fixed at the values iterated in this latter model, was included as well. Its center-shift value was forced to be 0.13 mm/s lower than that of the B-site doublets. These severe restrictions for the A-site component were required because of its weak contribution and the strong overlap with the dominant B-site component. Some relevant numerical results from this QSD procedure are presented in Table 2. For comparison, the goodness-of-fit values produced by the three-doublet fits, χ^2_{3d} , are listed as well. It is clear that the QSD approach consistently produces better fits than the three-doublet model, but not substantially so. With the exclusion of the center shift, all other parameters are not affected by the temperature, and the range of scatter in the numerical values is significantly smaller than that which is indicated in Table 1. The calculated distribution profiles are smooth and do not provide any indication whatsoever that two basically distinct B sites would be present in the structure. Instead, as quantitatively reflected in the small differences between the respective average quadrupole splittings ($\langle \Delta E_Q \rangle$) and the maximum-probability values ΔE_Q^m , the profiles are nearly symmetrically shaped. Finally, the correlation between δ and ΔE_Q is weak (see parameter c in Table 2) and believed to be of little physical significance.

At this point, it remains inconclusive which of the two approaches, *i.e.* the three-doublet fit or the QSD fit, is physically more justified. Considering the average composition of the compound being investigated, it is difficult to imagine that two structurally more or less distinct B sites can have formed, even in the event that clustering has occurred. The relatively large difference in ionic radii of Mn^{2+} and Zn^{2+} is instead expected to result in a wide range of local distortions of the oxygen octahedra containing the Fe probes. In that respect, a QSD seems to be more realistic than just two isolated doublets (see also RANCOURT, 1994). The observation that the two doublets adjusted to the franklinite MS exhibit quadrupole splittings close to the values found for the respective end-members would then be merely fortuitous.

Table 2. Some relevant Mössbauer parameters derived from fitting a superposition of an A-site quadrupole doublet with a model-independent, B-site quadrupole-splitting distribution to the paramagnetic spectra of franklinite at selected temperatures T : average and maximum-probability splittings $\langle \Delta E_Q \rangle$ and ΔE_Q^m , center shift δ^m corresponding to maximum probability, slope c of the linear correlation between center shift and quadrupole splitting, and relative spectral area A_f of the A-site contribution. The quantity χ^2 is the goodness-of-fit and χ^2_{3d} refers to the numerical analysis using one A-site and two B-site doublets.

T (K)	χ^2	χ^2_{3d}	$\langle \Delta E_Q \rangle$ (mm/s)	ΔE_Q^m (mm/s)	δ^m (mm/s)	c	A_f
265	446	465	0.435	0.407	0.378	-0.016	0.05
280	587	605	0.440	0.405	0.368	-0.017	0.05
300	507	537	0.436	0.410	0.356	-0.019	0.05
325	559	611	0.435	0.412	0.342	-0.018	0.06
350	578	609	0.434	0.416	0.327	-0.019	0.05
380	514	526	0.438	0.412	0.309	-0.017	0.05
410	569	617	0.439	0.418	0.291	-0.013	0.06
440	518	541	0.439	0.416	0.272	-0.010	0.07
470	497	557	0.442	0.418	0.253	-0.011	0.07

*Low-temperature Mössbauer spectra:
external field absent*

A set of representative low-temperature MS is reproduced in Fig. 2, showing the dramatic changes in line shape with increasing temperature. Synthetic (Me, Zn) ferrites, with Me as divalent cation, are known to undergo electronic relaxation effects that give rise to characteristic Mössbauer patterns at temperatures that are comparable to those covered in this study (see references cited in the review by VANDENBERGHE and DE GRAVE, 1989). It is clear that the line shapes observed here are markedly different from these reported patterns, implying that a simple collective relaxation process cannot explain these franklinite MS. A notable distinction from the relaxation spectra measured for the synthetic ferrites concerns the apparent splitting of the outer absorption lines (see Fig. 2 for $T = 80$ and 115 K) into two, well-separated components. Another peculiar feature is the appearance of seemingly extraneous peaks as clearly observed in the 80 K spectrum (see Fig. 2, at velocities of approximately -1.8 mm/s and 2.2 mm/s). Attempts to interpret the low-temperature MS ($30 \leq T \leq 230$ K) using a two-component, Blume-Tjon relaxation model (for a review and relevant references, see HOY, 1984) have remained unsuccessful so far.

Hence, it cannot be concluded whether the appearance of the two spectral components could be an indication for the existence of two kinds of clusters.

The spectra recorded at 4.2 K (see Fig. 2) and 9 K seem to present fewer challenges to their interpretation. However, they exhibit substantially asymmetric peak depths for corresponding pairs of lines, pointing at first glance to the presence of at least two distinct subspectra with different Mössbauer parameters. As it was experienced, the numerical interpretation of these MS is not straightforward, and several different physical approaches, described in the following paragraphs, have been considered in fitting the MS. The goodness-of-fit (χ^2) values, obtained under the various assumptions, are indicated in Table 3.

In a first attempt, two symmetrical sextets with equal line-width parameters were used to fit both spectra (model 2SS in Table 3). This model is the simplest one that could possibly produce results consistent with those of the three-doublet fits to the high-temperature MS, and hence with the suggestion of clustering. The values for the hyperfine fields, H_{hf} , and the quadrupole shifts, $2\epsilon_Q$, were iterated to be $H_{hf,1} = 501 \pm 2$ kOe and $2\epsilon_{Q,1} = -0.19 \pm 0.04$ mm/s, and $H_{hf,2} = 509 \pm 2$ kOe and $2\epsilon_{Q,2} = 0.13 \pm 0.03$ mm/s for the first and second components respectively. For both subspec-

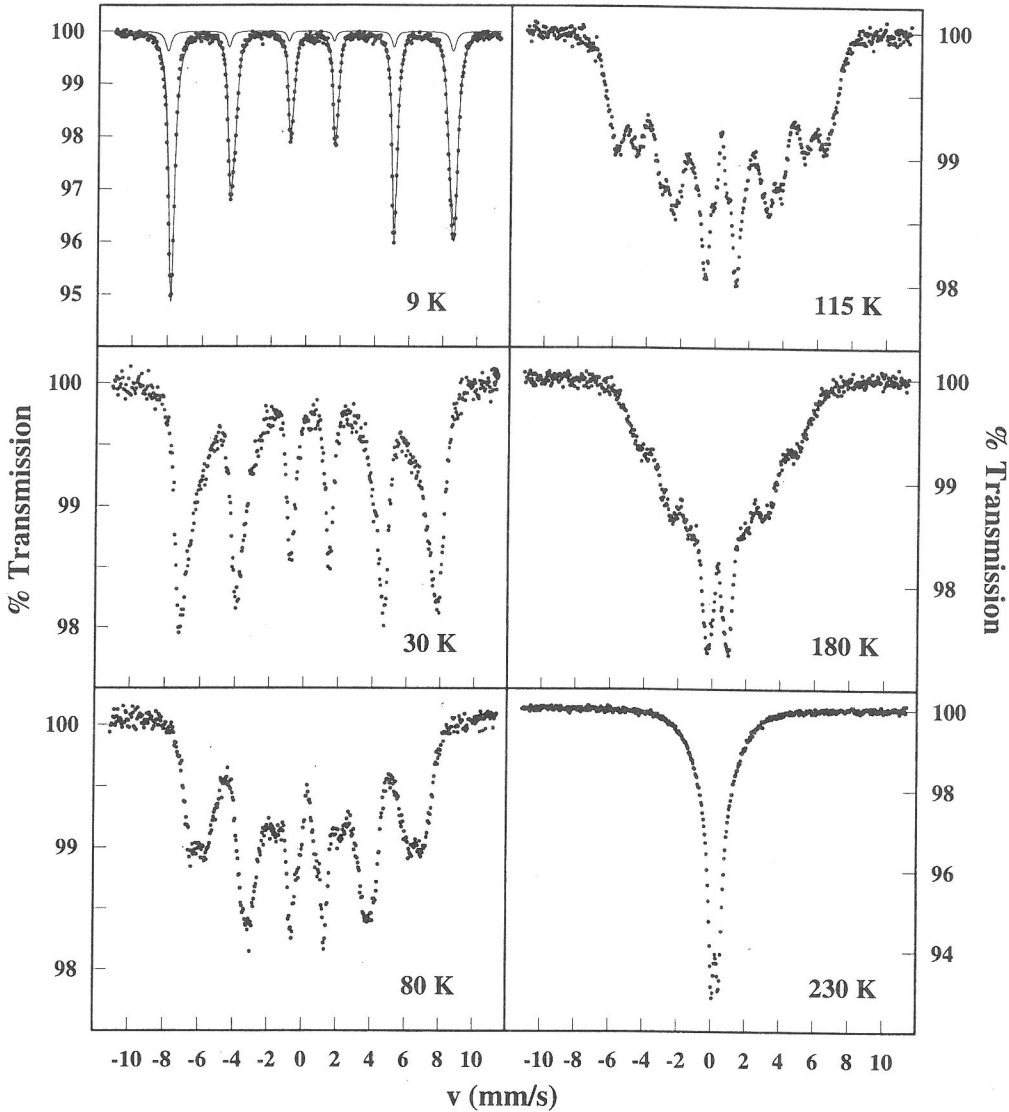


FIG. 2. Mössbauer spectra of franklinite at some selected low temperatures as indicated. The full line through the data points of the 9 K spectrum is the calculated spectrum using the asymmetrical line shape for the B-site pattern. The weak A-site sextet, assumed to be Lorentzian, is shown. The appearance of two components at intermediate temperatures (80 and 115 K) is obvious.

tra at 4.2 and 9 K, a value of 0.480 ± 0.006 mm/s for δ was obtained from the data, again typical for a six-fold coordination. In contrast to the paramagnetic spectra, the presence of a weak third component arising from tetrahedral Fe^{3+} ions could not be resolved straightforwardly from the magnetically-split MS. At this point, no further attempts were made to fit such a component with constraint parameter values.

If the clustering model is assumed to be real and responsible for the appearance of two magnetic components, then on the basis of the literature values of the hyperfine fields at 4.2 K for ZnFe_2O_4 and MnFe_2O_4 , viz. respectively 502 (VARRET *et al.*, 1971) and 513 to 517 kOe (MORRISH and CLARK, 1975), it would be logical to assign the component with the highest field to the Mn-rich clusters. However, this assignment is not consistent with the re-

Table 3. The goodness-of-fit χ^2 obtained for the various fitting models applied to interpret the B-site subpattern in the franklinite Mössbauer spectra recorded at 4.2 and 9 K. 2SS: two unconstrained symmetric sextets; 2SS1/1 and 2SS1/3: two symmetric sextets with area ratios 1/1 and 1/3 respectively; MHFD: a model-independent distribution of hyperfine fields; 1AS: one asymmetric sextet.

Model	$T = 4.2$ K	$T = 9$ K
2SS	1165	1252
2SS1/1	1193	1345
2SS1/3	1182	1671
MHFD	1047	1115
1AS	1040	948

sults derived from the paramagnetic spectra in the sense that the area ratio of the respective sextet components is found to be 60:40, while approximately the reverse number is obtained for the corresponding doublet components. Fixing the area ratio of the sextets to this latter number results in an increase of χ^2 by 35% (4.3 K) to 75% (9 K), with significant deviations between experimental and calculated line shapes.

Even if in the above 2SS model the assignment of the sextets is reversed, there remains an inconsistency, in particular with respect to the iterated $2\epsilon_Q$ values, that renders the model doubtful. Depending on the sign and the relative magnitudes of the anisotropy constants, the domains' spin direction, and hence that of the hyperfine fields, in cubic collinear ferrimagnets is along one of three crystallographic axes [100], [110], and [111] (SMIT and WIN, 1959). On the other hand, the principal axis of the electric field gradient (EFG) in spinel ferrites is generally along one of the four local [111] axes. Therefore, for a spin direction coinciding with [100], one sextet component with a shift $2\epsilon_Q = 0$ mm/s is expected. In contrast, a [111] orientation, as in MnFe_2O_4 (KÖNIG, 1971), leads to two sextets with $2\epsilon_Q$ values of respectively ΔE_Q and $-\Delta E_Q/3$, and with relative abundance of 1:3, while a [110] direction yields two sextets as well, however with shifts of $2\epsilon_Q = -\Delta E_Q/2$ or $\Delta E_Q/2$ and with equal area (DE GRAVE *et al.*, 1993). If in these two latter cases the observed spectrum is fitted as a single symmetrical component, the obtained

quadrupole shift will be close to zero. The two components resolved from the low-temperature MS irrefutably have non-zero quadrupole shifts. Hence, it may be concluded that the 2SS model as defined above produces results that are not in line with those derived from the doublet MS. Therefore it does not confirm the suggested clustering mechanism.

In a subsequent stage, and following the above reasoning with respect to the possible spin directions, only one physical component was considered, using two different hyperfine-field values as a result of the mentioned orientation effects. This difference is due to the dipolar-field contribution to H_{hf} , which shows a θ dependence similar to that referring to $2\epsilon_Q$ (DE GRAVE *et al.*, 1993). Both sextets were forced to have the same center shift and line-width parameters. Their relative areas were constrained according to the spin state: 1:1 (spins along [110], model 2SS1/1 in Table 3) or 1:3 (spins along [111], model 2SS1/3 in Table 3). An additional sextet, with fixed relative area of 0.06, and referring to A-site Fe^{3+} species, could be included in the fit; however its hyperfine parameters are highly unprecise. The resulting values for the hyperfine fields and quadrupole shifts of the two B-site subspectra, B1 and B2, at 4.3 and 9 K are listed in Table 4. The center shift was in the range 0.47–0.48 mm/s, and the outer line width was in the range 0.40–0.45 mm/s. As seen from Table 3, the agreement between experimental and calculated spectra has not improved compared to the 2SS approach. Consistent quadrupole splittings ΔE_Q (averaged for the 4.3 and 9 K runs) of -0.34 and -0.25 mm/s are calculated from the adjusted $2\epsilon_Q$ values (see Table 4) for respectively the 2SS1/1 and 2SS1/3 models. The magnitude of these splittings, in particular of the latter one, is rather low in view of the results derived from the quadrupole doublets, using for example a model-independent quadrupole-splitting distribution to fit these MS (note that the sign of ΔE_Q is undetermined from a quadrupole doublet). Otherwise, the calculated dipolar fields seem to possess reasonable values regardless of the applied approach. From the numerical data reported for MnFe_2O_4 by KÖNIG (1971), one can deduce $H_{\text{dip}} = -7.5$ kOe, which compares excellently with the present results. In conclusion, although both the 2SS1/1 and 2SS1/3 models are believed to have a more solid, physical background than the 2SS model, it remains unfeasible to express any preference towards either of the three models merely on the basis of the obtained fitting results.

Table 4. Hyperfine fields H_{hf} and quadrupole shifts $2\varepsilon_{\text{Q}}$ at 4.3 K and 9 K for the two symmetrical sextets B1 and B2 fitted to the experimental spectra in case the spins are assumed to be aligned along a domain's [110] crystallographic direction (model 2SS1/1) or along a [111] axis (model 2SS1/3). The relative area ratios were fixed at 1:1 and 1:3 respectively. H_{dip} is the dipolar field. In the 1AS model, only one B-site pattern, with asymmetric line shape, has been considered and the data contained in the fourth column refer to the quadrupole splitting ΔE_{Q} . The two bottom rows refer to the annealed franklinite sample.

Model	T (K)	$H_{\text{hf}}(\text{B1})$ (kOe)	$2\varepsilon_{\text{Q}}(\text{B1})$ (mm/s)	$H_{\text{hf}}(\text{B2})$ (kOe)	$2\varepsilon_{\text{Q}}(\text{B2})$ (mm/s)	H_{dip} (kOe)
2SS1/1	4.3	502	-0.17	508	0.17	-6
	9	503	-0.12	512	0.14	-8
2SS1/3	4.3	497	-0.24	508	0.07	-8
	9	501	-0.26	510	0.10	-7
1AS	4.3	505	-0.44			-8
	9	507	-0.42			-9
1AS	4.3	506	-0.42			-9
	9	507	-0.40			-10

For the matter of completeness, the 4.2 and 9 K spectra have also been analysed in a next step by a model-independent magnetic hyperfine field distribution (model MHFD), reflecting the non-uniqueness of the field as a result of fluctuations in the chemical environment of the probe iron nuclei (VANDENBERGHE *et al.*, 1994). The observed line shape was reasonably well reproduced, however not substantially better than in the case of the previous models (Table 3). Within the experimental uncertainties, the maximum-probability and the average field values were found to be equal, *i.e.* 506 and 505 kOe for $T = 4.3$, and 509 and 508 kOe for $T = 9$ K. Hence, the field distributions seem to be symmetrical. This finding is to some extent unexpected considering the fact that chemical disorder in spinel ferrites is known to commonly give rise to asymmetric distributions, even at 4.3 K and especially on the octahedral sites (SAWATZKY *et al.*, 1969). Finally, the two remaining models mentioned in Table 3 were inspired by the results of the applied-field Mössbauer measurements, and will be discussed in the next section.

Low-temperature Mössbauer spectra: applied field

A collection of applied-field Mössbauer spectra (AFMS) is presented in Fig.3. In contrast to what

one would expect for a collinear ferrimagnet in a strong, longitudinal external field H_{ext} , the middle lines ($\Delta m_{\text{I}} = 0$ nuclear transitions) have not vanished, meaning that the spins are not aligned along the direction of the applied field. The average canting clearly decreases with increasing field strength and, at a given field, with increasing temperature T . At 30 K in $H_{\text{ext}} = 60$ kOe, the canting has almost completely vanished. Since Mn^{2+} and Fe^{3+} are both S-state cations, and hence only poorly anisotropic, this canting is almost certainly not a result of the applied fields being too weak to dominate any preferred orientation of the net magnetic moment. Instead, the presence of the middle lines, and the changes of their intensities with changing T and H_{ext} , can be explained by the occurrence of so-called *locally canted spin states* (LCSS) (ROSEN-CWAIG, 1970). These LCSS arise from the selective magnetic dilution of the tetrahedral sublattice. B-site Fe^{3+} species with none or only a small number of magnetic A-site nearest-neighbours are subjected to a weak antiferromagnetic A-B superexchange interaction, while the B-B interaction, which opposes the ferrimagnetic alignment, is not affected. As a result, the corresponding B-site spins take on an orientation that does not coincide with the orientation of the domain's net magnetic moment, *i.e.* with the direction of H_{ext} . Higher temper-

atures and stronger fields reduce these LCSS. Such a magnetic structure is often termed *re-entrant ferrimagnetism* (BRAND *et al.*, 1985).

A second notable feature about the AFMS is the presence of a weak high-field component. As the numerical analyses of the spectra show (see later), this component at 4.3 K is partly due to tetrahedral Fe^{3+} ions, and partly to octahedral ones that have their spins reversed. Since the net B-site magnetic moment is higher than that of the A sites, the latter one is antiparallel to the external field and hence this field adds to the hyperfine field acting on the A sites and on the spin-reversed B sites. At 30 K, spin reversal has ceased to exist.

Finally, a third observation should be stressed. This concerns the asymmetric peak depths of corresponding pairs of absorption lines. This asymmetry is also obvious in the AFMS of synthetic (Mn, Zn) ferrites and was accounted for by MORRISH and CLARK (1975) by introducing in their fitting procedure two B-site patterns according to a different number of magnetic A-site neighbours (Mn^{2+}) to the probe iron nuclei. One can mention at least two arguments that question the full correctness of these authors' interpretation. First, for the composition range comparable with the presently studied franklinite, configurations consisting of $\text{Zn}_i\text{Mn}_{6-i}$ with $i = 5, 4, 3,$ and 2 all have a significant probability, so that three or four subpatterns would be required to reproduce the experimental line shape. Secondly, the fitted B-site center-shift values were found to differ by approximately 0.08 mm/s, and such a large difference is unlikely to be realistic.

Asymmetric B-site peak depths in AFMS of spinel ferrites are not unusual and occur even for members in which the B-site Fe atoms exhibit a unique nearest-neighbour A-site cation configuration such as magnetite and Co-substituted magnetites (DE GRAVE *et al.*, 1993; PERSOONS *et al.*, 1993) and maghemite (BOWEN *et al.*, 1994). The appearance of asymmetry is a consequence of the spin alignment along \vec{H}_{ext} . As a result, the angle θ between the spin direction and the EFG's principal axis becomes random, and due to the θ -dependence of the dipolar-field contribution, the hyperfine field becomes anisotropic. This anisotropy leads to an asymmetrical line shape which can be expressed analytically in the case of axial symmetry (DE GRAVE *et al.*, 1993). The full lines in the 4.3 K spectra as shown in Fig. 3 are the result of fitting such a line function to the B-site absorption (AS component). Because the weak-field component was featureless, a simple Lorentzian shape was assumed (LS component). The relative area of the

middle lines was allowed to vary, but it turned out to be small. It is therefore unclear whether or not all A-site spins are aligned along the direction opposite to that of the external field. A similar fitting procedure could successfully be applied for the (9 K, 60 kOe) spectrum (not presented in Fig. 3). In all cases, the observed AFMS are reasonably well reproduced by the adjusted ones, with minor deviations especially as far as the middle lines are concerned. These deviations are due to fluctuations on the magnitude H_{hf} of the hyperfine field and on the orientation, with respect to the propagation of the γ -rays, of the effective field \vec{H}_{eff} (*i.e.* the vectorial sum of the hyperfine and external fields) that determines the intensity of the ($\Delta m_I = 0$) transitions. This latter effect cannot be modelled analytically in the fitting routine. The non-unique strength of H_{hf} is reflected in the rather broad width obtained for the outer lines, *viz.* 0.45 mm/s.

The AFMS recorded at 14 K and 30 K could not be described adequately in the way mentioned in the preceding paragraph. In order to quantify some of their properties, a superposition of two, model-independent HFD was tentatively used, with effective-field values varying in the ranges 330–500 kOe and 550–600 kOe respectively, at steps of 3 kOe, for $T = 14\text{K}$, and 230–500 kOe and 500–600 kOe, at steps of 5 kOe, for $T = 30\text{K}$. For the most prominent component, asymmetrical elementary sextets, with adjustable line width Γ , were chosen. Center shift δ , dipolar-field contribution H_{dip} , quadrupole splitting ΔE_Q , and area ratios A_2/A_1 (second to first line) were all fitted. Lorentzian elementary quadruplets were considered for the weak high-field pattern (*i.e.* assuming zero canting), with adjustable δ value and quadrupole shift ϵ_Q fixed at zero.

Numerical data obtained from the fitting procedures applied to the AFMS are collected in Table 5. The dipolar-field value, being on the average -8 ± 2 kOe, and the center shift of the AS component are typical for octahedral Fe^{3+} in a spinel ferrite. The quadrupole splitting is found to be scattered within the range $\Delta E_Q = -0.44 \pm 0.03$ mm/s and is in excellent agreement with the average $\langle \Delta E_Q \rangle$ calculated from the paramagnetic spectra (see Table 2). Its sign is consistent with that found for ZnFe_2O_4 (EVANS *et al.*, 1971). The behavior of the relative line area parameter A_1/A_2 quantitatively confirms the reduction in spin canting with increasing applied-field strength and temperature, and hence supports the suggested LCSS mechanism. The variation of the fractional contribution A_{LS} reflects the gradual decrease of the number of re-

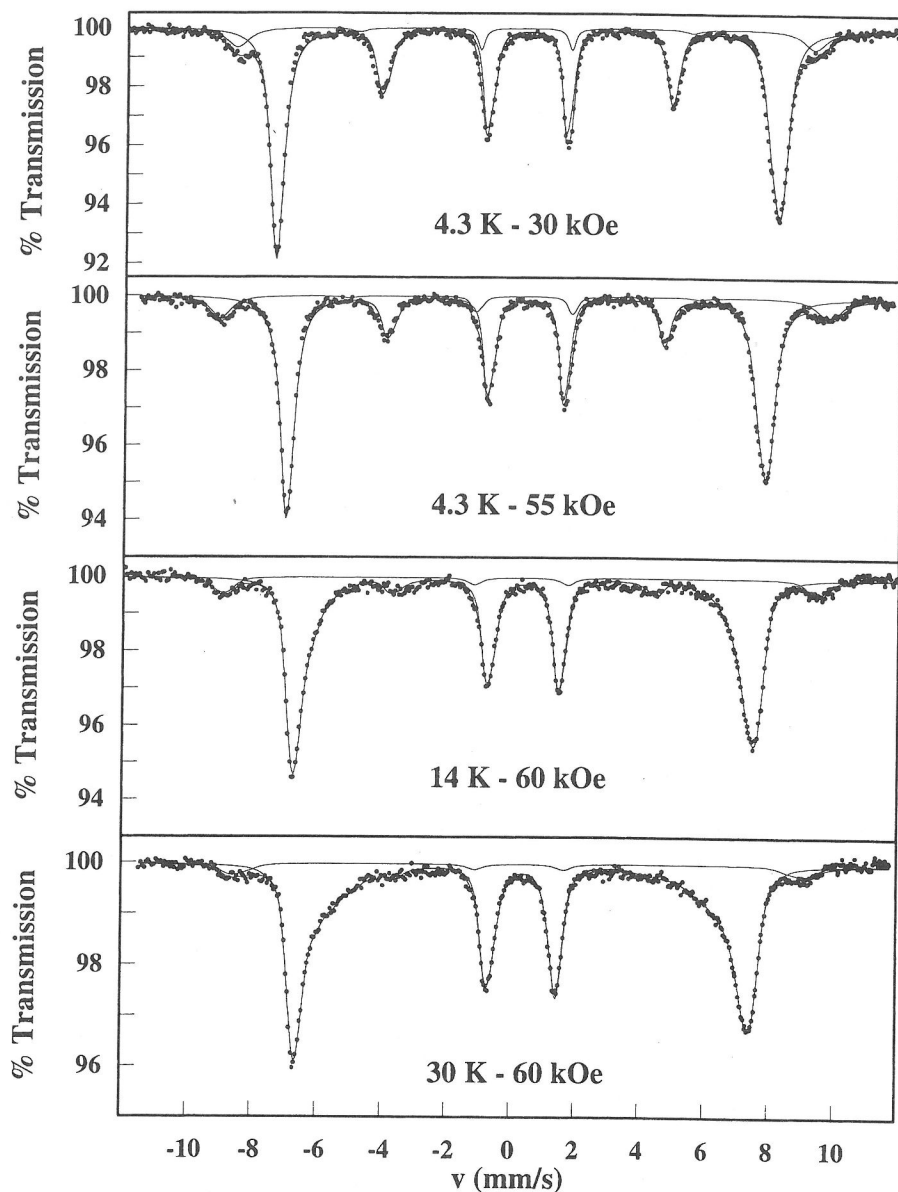


FIG. 3. Applied-field Mössbauer spectra of franklinite at field strengths and temperatures as indicated. The full lines are the calculated spectra using either a superposition of a symmetrical (high-field component) and an asymmetrical subpattern (4.3 K), or a superposition of two hyperfine-field distributions with an asymmetrical, elementary sextet for the B-site component (14 K and 30 K).

versed B-site spins as T increases, and the δ value for the LS component at 30 K indicates that this component can exclusively be attributed to tetrahedral Fe^{3+} . It proves that Fe is indeed present on the A sites and the A_{LS} value is in excellent accordance

with the results derived from the high-temperature MS (see Table 2, parameter A_i). In summary, the AFMS are consistent with the LCSS picture and their numerical interpretation has provided reasonable results for the various physical quantities,

Table 5. Some relevant Mössbauer parameters obtained from the external-field spectra of as-collected frankinite and of an annealed sample. A superposition of an asymmetrical sextet (AS) for the main component, and a Lorentzian sextet (LS) for the weak high-field component was used for the spectra corresponding to $T = 4.3$ and 9 K. For higher T values, the effective fields H_{eff} of both components were given a model-independent distribution. A_2/A_1 is the relative spectral area of the second line with respect to the first one, and A_{LS} is the fractional contribution of the LS component.

T (K)	----- AS -----						----- LS -----			
	H_{ext} (kOe)	H_{eff} (kOe)	H_{dip} (kOe)	δ (mm/s)	ΔE_{Q} (mm/s)	A_1/A_2	H_{eff} (kOe)	δ (mm/s)	A_1/A_2	A_{LS}
4.3	30	481	-6	0.47	-0.47	0.28	554	0.40	0.13	0.12
4.3	55	459	-6	0.48	-0.45	0.18	583	0.42	0.06	0.12
4.3*	60	451	-8	0.48	-0.46	0.10	577	0.41	0.04	0.14
9	60	443	-10	0.47	-0.41	0.10	578	0.41	0.11	0.09
14	60	442 [†]	-7	0.48	-0.46	0.07	557 [†]	0.38	0. [‡]	0.08
30	60	436 [†]	-8	0.48	-0.43	0.05	551 [†]	0.34	0. [‡]	0.07

[†]value corresponding to maximum probability

[‡]fixed in the iteration

*data referring to the annealed sample.

which are moreover completely in line with the data obtained from fitting the paramagnetic MS as a superposition of an A-site quadrupole doublet and a B-site QSD.

At this point, the zero-field MS recorded at 4.3 and 9 K need to be clarified. The interpretation is proposed to be as follows. Due to the LCSS in the octahedral sublattice, the angle θ between the hyperfine field and the EFG's principal axis varies from site to site, and a situation similar to that encountered when the absorber is subjected to a strong field can be suggested. Therefore, the B-site component is again fitted with an asymmetrical pattern with all parameters adjustable (model 1AS in Table 3). A Lorentzian shape is assumed for the A-sites, with all parameters, except the hyperfine field, fixed: $\delta = 0.34$ mm/s, $2\epsilon_{\text{Q}} = 0$ mm/s, and $A_1 = 0.07$. The fits are reasonable (see Table 3) and an example is shown in Fig. 2 for the 9 K spectrum. The relevant B-site parameters are included in Table 4, and are, as far as H_{dip} and ΔE_{Q} are concerned, in excellent agreement with the results derived from the AFMS. For the A-site hyperfine field, values of 511 and 514 kOe were iterated for $T = 4.3$ and 9 K respectively. This would mean that the A-

site hyperfine field is larger than the B-site one, which at first glance seems rather unusual for spinel ferrites (VANDENBERGHE and DE GRAVE, 1989). However, one can understand the observed feature for the present ferrite compound on the basis of the weaker supertransfer from Mn_A to Fe_B as compared to that from *e.g.* Fe_A to Fe_B , and the high number of nearest-neighbour B-site Fe^{3+} cations to any of the A-site probe nuclei, making the total supertransferred spin density from B to A sites relatively large.

A final point of discussion concerns the magnitudes of the B-site hyperfine fields H_{hf} as obtained from the zero-field MS and of the effective fields H_{eff} derived from the AFMS. The relation between these two quantities is generally given by:

$$H_{\text{eff}}^2 = H_{\text{ext}}^2 + H_{\text{hf}}^2 - 2H_{\text{hf}}H_{\text{ext}} \cos \alpha \quad (1)$$

α being the angle between the γ -ray direction (*i.e.* the direction of H_{ext}) and the spin direction. The (average) canting α can be determined from the area ratio A_1/A_2 as defined earlier:

$$\alpha = \arcsin \left[\frac{1.5 A_2/A_1}{1 + 0.75A_2/A_1} \right]^{1/2} \quad (2)$$

Using the data for A_1/A_2 as listed in Table 5 and referring to the 4.3 K spectra, canting angles of 36° and 29° are calculated for applied fields of 30 and 55 kOe respectively. Subsequently, from the H_{hf} values of Table 4, eqn.(1) yields for H_{eff} 481 and 458 kOe respectively, in agreement with the experimental results (see Table 5). Finally, it should be stressed that similar calculations for the A-site components cannot be performed, firstly because this component in the AFMS cannot be distinguished from the B-site reversed-spin component, and secondly because no information is available about the A-site canting and dipolar-field contribution.

Annealed sample

According to VOGEL *et al.* (1976), the changes in the RT Mössbauer line shape upon annealing their sample (indicated composition $\text{Zn}_{0.730}\text{Mn}_{0.346}\text{Fe}_{1.924}\text{O}_4$) provide an indication that some kind of ordering is present in the as-collected franklinite. For the present sample, annealing was not found to produce any significant visible effect on the MS recorded at RT, 9 K and 4.3 K, without an externally applied field and at 4.3 K in a 60 kOe field. The RT doublet, when fitted with a QSD for the B-site component, has an average quadrupole splitting of 0.48 mm/s, and a maximum-probability value of 0.44 mm/s. Both quantities are about 10% larger than the results for the parent material (see Table 2), as is the width of the distribution ($1x\sigma$ of 0.23 mm/s as compared to 0.20 mm/s for the non-annealed mineral at RT). These differences might be considered significant, suggesting increased deformations of the structural and/or surrounding-charge symmetries of the Fe-containing octahedra. A slight rearrangement of the cation distribution could indeed explain such a behavior. The relative spectral area of the A-site component, *i.e.* 0.055, was found to have remained unchanged upon annealing. Concerning the low-temperature MS of the annealed sample, the same trends in the goodness-of-fit χ^2 were obtained when fitting the various models as discussed in the preceding sections. Some results of the numerical analyses based on a asymmetrical B-site line shape are included in Tables 4 and 5. It is obvious that none of the involved parameters has markedly changed, implying that the annealing, and the possible alteration of the cation distribution resulting from it, has but a little effect on the low-temperature magnetic structure.

CONCLUSIONS

Both the paramagnetic doublet spectra and the low-temperature, magnetically split spectra (in particular those recorded with the absorber subjected to the external fields) consistently reveal that in the investigated franklinite mineral about 0.06 Fe atoms per formula unit are located in the tetrahedral sublattice. The high-temperature spectra could not detect any significant amount of Fe^{2+} and are adequately described as a superposition of an A-site doublet and two B-site doublets. The fitted quadrupole-splitting values of these latter two are close to the literature values reported for Zn and Mn ferrite respectively. This finding could be related to the suggested presence of Mn-rich and Zn-rich clusters. However, slightly but consistently better fits were obtained using an A-site doublet and a quasi-continuous quadrupole-splitting distribution for the B sites. All parameters except the center shift remain remarkably constant as the temperature varies. The average quadrupole splitting is found to be within the range 0.438 ± 0.004 mm/s. This fitting model does not provide any support in favor of the cluster formation.

At temperatures below 245 K and down to ≈ 20 K, the spectral shape is governed by relaxation effects. The relaxation process seems to be unusual in the sense that it is not a collective one. Instead, two clearly separated subpatterns emerge. A two-component Blume-Tjon model is unsuccessful at describing the observed line shapes in all details. The spectra recorded at 4.3 and 9 K seem to be free from relaxation effects, but clearly exhibit significant asymmetry in peak depths for corresponding pairs of lines. In view of the suggested clustering, two symmetrical B-site sextets were fitted to these spectra. The results were found to be inconsistent with those obtained in the paramagnetic regime. Two other models, assuming the spins to be aligned along a domain's [111] or [110] crystallographic axis respectively, were unsuccessful as well. A similar conclusion was arrived at with respect to a model-independent magnetic hyperfine field distribution.

Applied-field Mössbauer spectra recorded at 4.3 and 9 K reveal the existence of locally canted spin states and reversed B-site spins. Both phenomena ceased to exist at a temperature in the vicinity of 30 K and are characteristic for a re-entrant ferrimagnetic structure. The predominant B-site subpattern again is asymmetrical and could be reproduced adequately by a line shape calculated on the basis of a random angle between the hyperfine field and

the EFG's principal axis. An additional distribution on the effective hyperfine fields was introduced to interpret the AFMS at 14 and 30 K. The models allowed the determination of the dipolar contribution to the B-site magnetic hyperfine field which was found to be -8 ± 2 kOe. The B-site quadrupole splitting was found to be negative and its magnitude is in excellent agreement with the average value of the QSD fitted to the paramagnetic spectra. The existence of LCSS at low temperatures implies that in zero applied field the angle between the B-site hyperfine field and the EFG's principal axis is also fluctuating, so that the asymmetry in the corresponding spectra can be explained accordingly. Using one asymmetrical B-site pattern and a constrained Lorentzian A-site sextet, the MS at 4.3 and 9 K were reproduced adequately, with parameter values that are in line with the results derived from the AFMS. As a final conclusion, it may be inferred that there appears to be no need to assume the formation of Mn- and Zn-rich clusters in order to explain the MS observed for the investigated franklinite mineral. The present results furthermore raise some questions regarding the correctness of earlier reported interpretations of MS, obtained for synthetic (Mn,Zn) ferrites, in terms of possible nearest-neighbor A-site cation configurations.

Acknowledgements—The authors wish to thank Dr. R. P. Kruk (Jagiellonian University, Krakow) for his assistance with the interpretation of the relaxational Mössbauer spectra. This work was supported by the Fund for Joint Basic Research, Belgium (Grants No. 32.0014.93 and No. 32.0055.93).

REFERENCES

- BOWEN L. H., DE GRAVE E. and BRYAN A. M. (1994) Mössbauer studies in an external field of well-crystallized Al-maghemites made from hematite. *Hyperfine Interact.* **94**, 1977–1982.
- BRAND R. A., GEORGES-GIBERT H., HUBSCH J. and HELLER J.A. (1985) Ferrimagnetic to spin glass transition in the mixed spinel $Mg_{1+x}Fe_{2-2x}Ti_xO_4$: a Mössbauer and DC susceptibility study. *J. Phys. F: Met. Phys.* **15**, 1987–2007.
- DA COSTA G. M., DE GRAVE E., BOWEN L. H., VANDENBERGHE R. E. and DE BAKKER P. M. A. (1994) The center shift in Mössbauer spectra of maghemite and aluminum maghemites. *Clays Clay Minerals* **42**, 628–633.
- DE GRAVE E. and VAN ALBOOM A. (1991) Evaluation of ferrous and ferric Mössbauer fractions. *Phys. Chem. Minerals* **18**, 337–342.
- DE GRAVE E. and VOCHTEN R. (1985) An ^{57}Fe Mössbauer effect study of ankerite. *Phys. Chem. Minerals* **12**, 108–113.
- DE GRAVE E., PERSOONS R. M., VANDENBERGHE R. E. and DE BAKKER P. M. A. (1993) Mössbauer study of the high-temperature phase of Co-substituted magnetites, $Co_xFe_{3-x}O_4$. I. $x \leq 0.04$. *Phys. Rev. B* **47**, 5881–5893. (with Erratum, *ibid.* **48**, 3581.)
- EVANS B. J., HAFNER S. S. and WEBER H. P. (1971) Electric field gradients at ^{57}Fe in $ZnFe_2O_4$ and $CdFe_2O_4$. *J. Chem. Phys.* **55**, 5282–5288.
- HOY G. R. (1984) Relaxation phenomena for chemists. In *Mössbauer Spectroscopy Applied to Inorganic Chemistry* (ed. G. J. LONG), Vol. 1, Chap. 8, pp. 195–226. Plenum Press.
- KÖNIG U. (1971) Note on the Mössbauer effect in $MnFe_2O_4$. *Solid State Commun.* **9**, 425–427.
- KÖNIG U. (1972) Die magnetische Ordnung in Mangan-Zink-Ferriten. *Techn. Mitt. Krupp, Forsch.-Ber.* **30**, 1–14.
- METSGER R. W., TENNANT C. B. and RODDA J. L. (1958) Geochemistry of the Sterling Hill zinc deposit, Sussex County, New Jersey. *Bull. Geol. Soc. Am.* **69**, 775–788.
- MORRISH A. H. and CLARK P. E. (1975) High-field Mössbauer study of manganese-zinc ferrites. *Phys. Rev. B* **11**, 278–286.
- PERSOONS R. M., DE GRAVE E., DE BAKKER P. M. A. and VANDENBERGHE R. E. (1993) Mössbauer study of the high-temperature phase of Co-substituted magnetites, $Co_xFe_{3-x}O_4$. II. $x \geq 0.1$. *Phys. Rev. B* **47**, 5894–5905.
- RANCOURT D. G. (1994) Mössbauer spectroscopy of minerals. I. Inadequacy of Lorentzian-line doublets in fitting spectra arising from quadrupole splitting distributions. *Phys. Chem. Minerals* **21**, 244–249.
- ROSENCWAIG A. (1970) Localized canting model for substituted ferrimagnets. I. Singly substituted YIG systems. *Can. J. Phys.* **48**, 2857–2867.
- SAWATZKY G. A., VAN DER WOUDE F. and MORRISH A. H. (1969) Mössbauer study of several ferrimagnetic spinels. *Phys. Rev.* **187**, 747–757.
- SMIT J. and WIJN H. P. J. (1959) *Ferrites*. Philips' Technical Library.
- VANDENBERGHE R. E. and DE GRAVE E. (1989) Mössbauer studies of oxidic spinels. In *Mössbauer Spectroscopy Applied to Inorganic Chemistry* (eds. G. J. LONG and F. GRANDJEAN), Vol. 3, Chap. 3, pp. 59–182. Plenum Press.
- VANDENBERGHE R. E., DE GRAVE E. and DE BAKKER P. M. A. (1994) On the methodology of the analysis of Mössbauer spectra. *Hyperfine Interact.* **83**, 29–49.
- VARRET F., GERARD A. and IMBERT P. (1971) Magnetic field distribution analysis of the broadened Mössbauer spectra of zinc ferrite. *Phys. Status Solidi (b)* **43**, 723–730.
- VOGEL R. H., EVANS B. J. and SWARTZENDRUBER L. J. (1976) Intra site cation ordering and clustering in natural Mn-Zn ferrites. In *AIP Conf. Proc. No 34—Magnetism and Magnetic Materials* (eds. J. J. BECKER and G. H. LANDER), pp. 125–127. American Institute of Physics.